Excitation of ion-wave wakefield by the resonant absorption of a short pulsed microwave with plasma

Md. Kamal-Al-Hassan, Mikhail Starodubtsev, Hiroaki Ito, Noboru Yugami, and Yasushi Nishida
Department of Energy and Environmental Science, Graduate School of Engineering, Utsunomiya University, 7-1-2 Yoto, Utsunomiya, Tochigi 321-8585, Japan

(Received 17 February 2003; published 29 September 2003)

Unmagnetized, inhomogeneous laboratory plasma irradiated by a high power ($\eta = E_0^2/4\pi n_e kT_e \approx 5.0 \times 10^{-2}$) short pulsed microwave with pulse length of the order of ion-plasma period ($\tau_{pi} \lesssim 2\pi/\omega_{pi}$) is studied. Large density perturbation traveling through the underdense plasma with a velocity much greater than the ion sound speed produced by the resonant absorption of the microwave pulse has been observed. In the beginning the density perturbation has large amplitude ($\delta n/n_0 \approx 40\%$) and propagates with a velocity of the order of 10^6 cm/s. But later its amplitude as well as the velocity decrease rapidly, and finally the velocity arrives with twice the ion sound speed. The oscillating incident electromagnetic waves enhance highly localized electric field by the resonant absorption process and develop time-averaged force field which pushes plasma electrons from the resonant layer. As the electrons are accelerated to be ejected, they pull plasma ions as a bunch with them by means of self-consistent Coulomb force. This suprathermal ion bunch can excite an ion-wave wakefield.

DOI: 10.1103/PhysRevE.68.036404 PACS number(s): 52.35.Mw, 52.35.Fp, 52.40.Db, 52.90.+z

I. INTRODUCTION

An interesting topic in modern plasma physics is plasma based accelerators and plasma wakefield phenomena. Since the first proposal by Tajima and Dawson [1], many successful phenomena have been demonstrated in this area. Some new accelerator schemes [2–4] have been proposed and successfully demonstrated in proof-of-principles experiments. Plasma waves in the plasma wakefield accelerator (PWFA) are driven by one or more electron bunches. In the plasma wakefield accelerator concepts [5–8], plasma waves wakefield are excited by relativistic electron bunches, in which the electron beam should be terminated in a time shorter than the plasma wave period (ω_{pe}^{-1}). When the beam density approaches one-half the plasma density, the excited electron plasma wave approaches the nonrelativistic wave-breaking limit to give the electric field $E \rightarrow \omega_{pe} mc/e$. Jones and Keinigs [9] described the possibility to excite ion waves by using an ion bunch with proper falloff time. Using an ion with mass M may increase the limiting electric field for fixed ω_{pe} by the ratio of the ion mass to the electron mass M/m. It has been shown that the optimal falloff time (τ_{fall}) of the driving beam depends on the plasma frequency as $\omega_{pe} = \tau_{fall}^{-1}$. However, in the case of ion movement, the ambipolar field limits the maximum field strength to be smaller than the case of electron bunch wakefield. Nishida *et al.* [10] have successfully excited the wake field in the ion-wave regime with a variety of shapes of ion bunches injected into a plasma in the double plasma machine. The experimental results show that a ramp-shaped ion bunch with a sharp falloff time can excite a large amplitude wakefield with $dn/n_0 \approx 17\%$. The amplitude of the wakefield decreases with an increase of falloff time constant of the incident ion bunch, along with the oscillation of amplitude. Experiment by Aossey *et al.* [11] has demonstrated plasma wakefield excitation in both a positive ion-electron plasma and a positive ion-negative ion-electron plasma system.

The main difficulty when exciting an ion wakefield is to produce sharp ion bunch shape with a proper falloff time. One of the possible ways to meet this requirement is to expel quickly the plasma electrons out from a small plasma region leaving behind a bare ion column. Resulting ambipolar electric field can accelerate plasma ions producing a short energetic ion bunch. In the present experiment we have produced an ion bunch with sharp falloff time by the above method using the resonant absorption process to expel plasma electrons from the resonant plasma layer. Indeed, a nonuniform unmagnetized plasma has been irradiated by a short microwave pulse with its duration shorter than the ion oscillation period ($\tau_{pi} = 2\pi/\omega_{pi}$). The key to excite strong wakefield is that the microwave pulse width should be of the order of ion oscillation period ($\tau_{pi} = 2\pi/\omega_{pi}$). The physical aspects are straightforward. The ponderomotive force created at the resonant area pushes out the electrons from that area, leaving behind bare ions. These ions are accelerated as an energetic ion bunch by the ambipolar force. Typical ion energy in a bunch has been measured to be about 58 eV, which is more than 100 times greater than the thermal ion. This suprathermal high energy ion bunch acts as the driving bunch to excite ion wakefield in the present experiment. The typical ion-plasma period $\tau_{pi} \approx 95$ ns is estimated by using the resonant density parameter ($n_c = 1 \times 10^{11}$ cm^{-3}) at the critical layer in the argon plasma-microwave interactions. The wakefield excited by the incident microwave of pulse width 85–90 ns is described in the experimental results. The maximum amplitude of the wakefield is observed about $\delta n/n_0 = 40\%$.

This paper is organized as follows. The experimental setup is described in Sec. II, results are presented in Sec. III, and Sec. IV discusses the results in the view of different theoretical aspects. Finally, the results of the paper are concluded in Sec. V.

II. EXPERIMENTAL ARRANGEMENTS

A schematic drawing of the experimental arrangements is shown in Fig. 1(a). A cylindrical, unmagnetized, nonuniform,

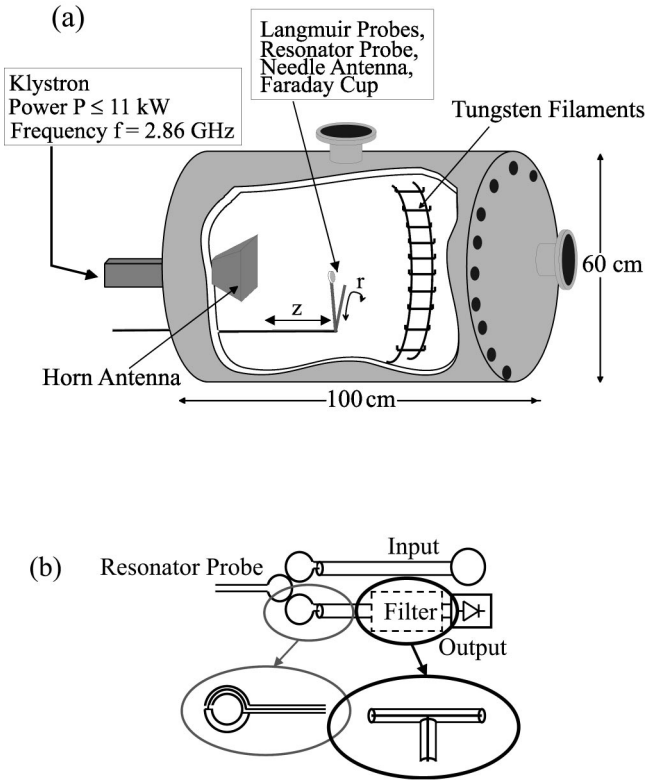

FIG. 1. Schematic drawing of (a) the experimental arrangements and (b) the microwave resonator probe.

argon plasma is produced in a stainless steel chamber 100 cm in length and 60 cm in diameter. The outside surface of the vacuum chamber is covered with line cusp arrangements for improved plasma confinement, made from permanent magnets having surface magnetic field strength of 4 kG. Plasma is produced by the pulsed discharge with applied voltage (60 V) between tungsten filament arranged as a cathode (heating current up to 95 A) and grounding chamber wall as anode with discharge duration 2 msec and repetition rate 10 Hz. The vacuum chamber is initially evacuated to a pressure $p \approx 2.5\times10^{-6}$ Torr and after filling argon gas, chamber pressure is adjusted to $p\approx6.5\times10^{-4}$ Torr. A *p*-polarized microwave pulse with frequency $f=\omega/2\pi=2.86$ GHz (corresponding critical plasma density $n_c=1\times10^{11}$ cm^{-3} for resonance absorption) and maximum power 11 kW is launched into the plasma from a rectangular horn antenna located at the lower plasma density side. The horn antenna has a metallic lens in order to minimize diverging output radiation angle for creating *p*-polarized microwave. The interaction area is located near or around the central axis of the chamber. To prevent the maximum reflection of the launched electromagnetic wave from the chamber walls, we have put glass wool inside the chamber walls in order to absorb the electromagnetic wave. The width of the microwave pulse is maintained from 80 ns to 250 ns with the full width at half maximum with a repetition rate of 10 Hz, and with typical falloff time (τ_{fall}) ranging from 85 ns to 200 ns, where τ_{fall} is the time difference between 10% and 90% of the maximum value of the microwave power. Plasma density as well as fluctuating wave forms are diagnosed by two disc shaped

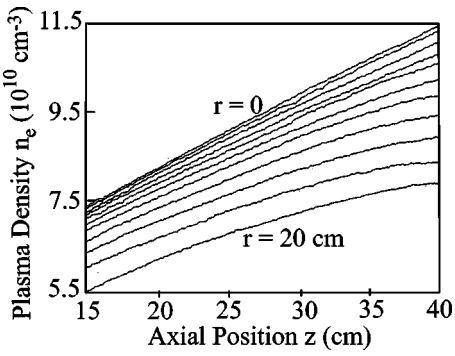

FIG. 2. Spatial density profiles inside the plasma chamber in the absence of incident microwaves. Each line is separated by 2 cm from neighboring lines.

(1 mm diameter) Langmuir probes, one facing towards the resonant region and the other facing opposite to the resonant region. A microwave resonator probe [12] is also used to measure plasma density. The schematic drawing of the microwave resonator probe is shown in Fig. 1(b). A U-shaped quarter wavelength resonator probe is coupled by two loop antennas in this device. A cylindrical needle antenna with a tip 2 mm in length and 0.25 mm in diameter is used to measure the spatial distribution of microwave field inside the plasma. A small Faraday cup of 23 mm in length and 10 mm in diameter is used to detect the energetic ion flux, flowing down the lower density region from the resonant layer. All three electrodes of this energy analyzer (two grids and one collector) are covered with a copper cup to shield them from microwave and other noises. All diagnostic tools are movable in the axial *z* direction and rotatable in the radial *r* direction by a low power DC motor system.

III. EXPERIMENTAL RESULTS

When a short *p*-polarized microwave pulse with a frequency ω is irradiated in an inhomogeneous plasma, the resonance absorption occurs at the critical layer where $\omega=\omega_{pe}$. Figure 2 shows the spatial density profiles inside the plasma chamber in the absence of incident microwaves. A nonuniform plasma density of the order of 10^{10}–10^{11} cm^{-3} is observed. The density gradient scale length in the axial (z) direction at $r\approx5$ cm and radial (r) direction at $z\approx32$ cm are observed as $L_z\approx68$ cm and $L_r\approx52$ cm, respectively, where $r=0$ is the point on the chamber axis and $z=0$ is the point on the face of horn antenna, and plasma density increases as z. Electron temperature $T_e\approx3$ eV and ion temperature $T_i\approx0.5$ eV are observed to be approximately identical throughout the main part of the plasma volume, where the experiments are performed. After irradiating the microwave pulse with the plasma, a typical example of the microwave field in the resonant plasma obtained by a needle antenna coupled to a crystal detector is shown in Fig. 3(a). Figure 3(a) displays an axial profile of the microwave field at $r\simeq5$ cm. One can observe the resonantly excited field at about $z\simeq32$ cm, which is the position where the plasma density becomes critical one ($\approx1\times10^{11}$ cm^{-3}). It is seen that the microwave radiation vanishes beyond $z\simeq32$ cm over

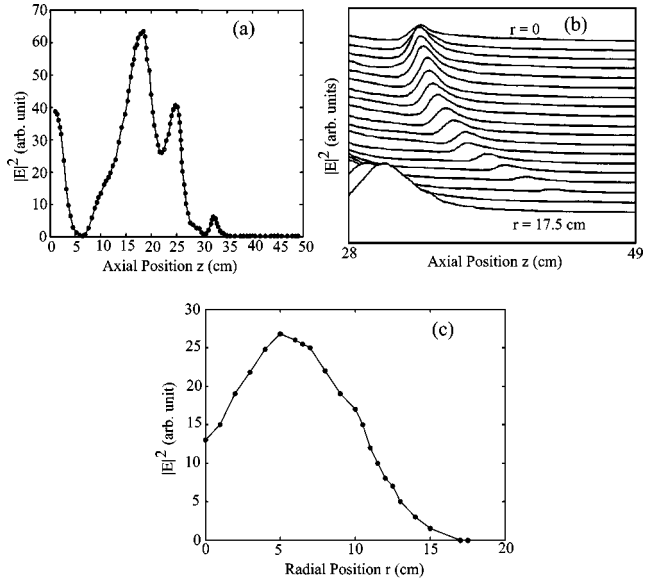

FIG. 3. (a) Axial profile of the microwave electric field inside the plasma at $r \simeq 5$ cm, (b) axial profiles of the resonantly excited electric fields inside the plasma for $r=0$ to $r=+17.5$ cm, and (c) amplitude profile of the resonant electric field intensity at different radial positions.

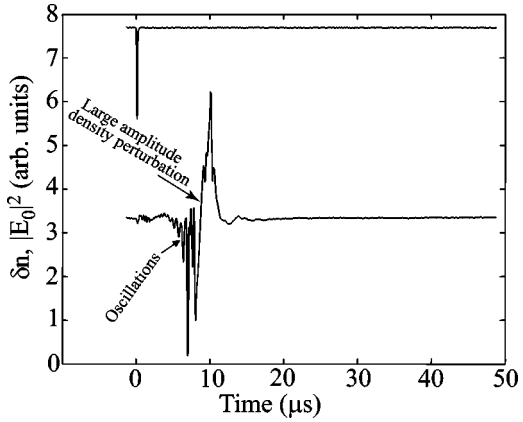

FIG. 4. The top trace represents the incident microwave pulse measured by needle antenna and the bottom trace represents the density perturbation measured by Langmuir probe as a function of time.

which the plasma becomes overdense. The peak at $z \approx 25$ cm is expected to be the peak which occurs near the reflection layer of the incident EM wave, where plasma density should be satisfied as $n_e \simeq n_c \cos^2\theta$. In the region $z < 25$ cm the standing wave pattern (for example, the peaks at $z \approx 18$ and 1 cm) is observed, but it differs from the well-known Airy function due to complicated geometry of the present experimental system. Indeed, the observed standing wave pattern is formed as a result of multiple wave reflections from the cutoff (reflection) plasma layer as well as the walls of the vacuum chamber. Figure 3(b) shows axial profiles of the resonantly excited peaks at different radial positions (from $r=0$ to $r=+17.5$ cm). If we consider the profiles from $r=-17.5$ cm to $r=+17.5$ cm, one can observe a typical two-dimensional parabolic profile of the resonant layer in the chamber. Figure 3(c) displays the amplitude profile of the resonant electric field at different r positions inside the chamber. Note that the maximal resonant field intensity occurs at $r \simeq 5$ cm and it decreases near the axis of the plasma column as well as for $r > 5$ cm. From Figs. 3(a) and 3(c) one can conclude that the maximum resonant field intensity is observed at $z \simeq 32$ cm and $r \simeq 5$ cm. Using the above experimental results one can obtain the angle of incidence by using the following equation [13] (which is also discussed in Sec. IV):

$$2\cos^2\theta = 1 + \frac{z_l}{L_z} \pm \left[\left(1 - \frac{z_l}{L_z} \right)^2 - \left(\frac{r}{L_z} \right)^2 \right]^{1/2}, \qquad (1)$$

where z_l is the microwave launching point inside the chamber. There are two roots of $\cos\theta$ in Eq. (1). With measured values $z_l = 1$ cm, $L_z = 68$ cm, $r=5$ cm, one obtains $\theta = 2.12°$ considering the plus sign and $\theta = 82.7°$ for minus sign. Out of these two roots, one can accept reasonable value $\theta = 2.12°$. From the above measurements, we can conclude that our process to locate maximum resonant point is reasonable.

Figure 4 shows typical oscillogram measured in the underdense plasma near the resonant layer. It should be mentioned that the time reference point at $t=0$ corresponds to the turning off of the microwave pulse throughout the paper. Density perturbations are measured by a disc Langmuir probe facing towards the resonant region and biased at the electron saturation current. We can easily distinguish two different phenomena observed in the bottom trace of Fig. 4: the higher frequency low amplitude oscillations and lower frequency high amplitude gross density perturbation. The former fluctuation may be due to the sheath instability and the lower frequency plasma density perturbation may come from wakefield effect. Let us first discuss the process of the sheath instability. This effect appears as high frequency oscillations in the electron saturation current with their characteristic frequencies about a few MHz. The instability occurs when a disc Langmuir probe is irradiated by accelerated ions produced during the resonant absorption. To illustrate the characteristics of this higher frequency oscillations we have measured plasma density perturbations by the microwave resonator probe and compared the results with Langmuir probe measurement as they are shown in Fig. 5. The vacuum resonance frequency of the microwave resonator is $f_0 = 4.88$ GHz and its quality factor $Q \approx 170$. A quarter wavelength filter rejects a large amplitude pick-up through the pump microwave at $f_{pump} = 2.86$ GHz. The probe is tuned to the slope of the resonance characteristics, thus the changing of the resonance frequency caused by the density perturbations would be proportional to the plasma density variation. In Figure 5 top traces show the density perturbation measured by the Langmuir probe and bottom traces the density perturbation measured by the microwave resonator probe. One can clearly notice the differences between the two results: the Langmuir probe signals show the existence of high frequency oscillations while the resonator probe measurements do not show them. Far from the resonance region (z

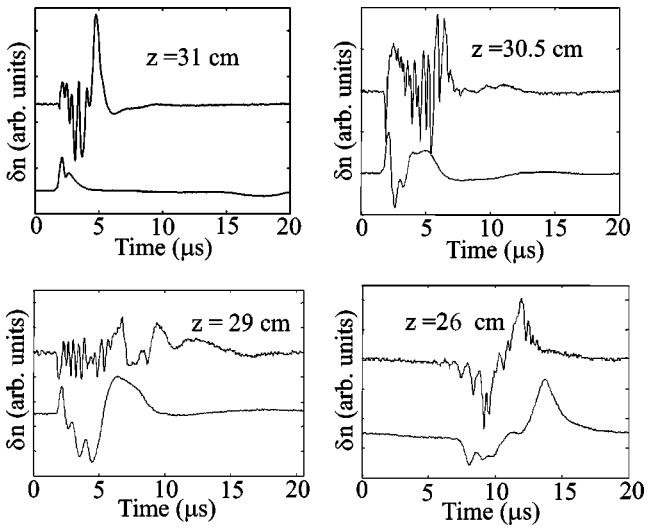

FIG. 5. The measurements of the density perturbation in above four graphs measured in different *z* positions by the Langmuir probe is shown in top trace and by the resonator probe is shown in bottom trace as a function of time.

=26 cm shown in Fig. 5) when the sheath instability disappears, the density perturbations measured by both the Langmuir probe and the resonator probe are very similar. This effect has not been observed at the ion saturation current as well as when the disc Langmuir probe is facing opposite to the resonant region (i.e., when accelerated ions do not interact with the probe surface). The instability occurs only when the probe is biased positively with respect to the plasma. The observed phenomena taken by both the Langmuir probe and resonator probe tell us that the higher frequency oscillations in the electron saturation current are not due to the plasma density fluctuations but are related to the sheath instability. The observed higher frequency oscillations of the electron saturation current take place when an energetic ion beam component comes into the sheath area of the biased probe. It does not represent the macro plasma density perturbation. It is an instability created by high energy suprathermal ion flux which is shot out by the nonlinear ponderomotive force developed in the resonant plasma region. We wish to suggest a simple physical model of the observed instability. Consider a positively biased (at U_0) probe immersed in the plasma with an ion beam (eU_b-beam energy). If $U_0 > U_b$, the beam will reflect back inside the electron-reach sheath. Near the reflection point its density increases manifold and, as a consequence, the total negative space charge of the sheath diminishes. As a result, an overshoot of the electron saturation current occurs due to the fact that the plasma ions do not evacuate instantaneously (recall that $v_b \gg c_s$ from the present experimental data, where v_b and c_s are the beam velocity and the ion sound speed, respectively). The duration of the overshoot corresponds to the time ($t_s \approx r_s/c_s \approx 0.12$ μs) taken by the plasma ions to move with the ion sound speed ($c_s \approx 2.5\times 10^5$ cm/s) across the sheath region ($r_s \approx 5\lambda_D \approx 0.3$ mm). Before plasma ions can move, the positive probe potential strongly penetrates into the plasma and in turn influences the ion beam. While the beam front has propagated toward the probe through potential-free plasma, the subsequent part of the beam propagates into sheath through a decelerating potential. Hence, the ion beam disruption occurs due to the time-of-flight effect and beam density inside the sheath decreases leading the sheath back to its initial unperturbed state.

Resonant absorption process and expulsion of plasma particles out of the resonant region cause large-amplitude density perturbations shown in Fig. 4, which has been found to propagate down the plasma density gradient as a nonlinear ion-wave. Here we will discuss physical origin and dynamics of these density perturbations. It has been observed that if we reduce the microwave pulse width (which also reduces the fall time τ_{fall}) to 85 ns, which is almost the same or even less than the ion oscillation period $\tau_{pi} = 2\pi/\omega_{pi} \approx 95$ ns, the instability part reduces considerably, while the amplitude of the density perturbation increases, such as shown in Fig. 6. Figure 6(a) displays the typical examples of the density perturbations as a function of time. The top trace shows the case with the microwave pulse width at 85 ns, middle trace at 150 ns, and bottom trace at 180 ns. One can see that the increase of the pulse width increases the sheath instability but decreases the amplitude of density perturbations as mentioned above. Figure 6(b) shows the variation of the amplitude of the density perturbations as a function of the incident microwave pulse width. One can see that the decrease of microwave pulse width (which decreases along with τ_{fall}) increases the density perturbations.

Now we are interested in showing the view of affected plasma density after irradiating the microwave pulse into the plasma. Figure 7 shows the spatial profiles of perturbed density along the axial *z* direction at $r \simeq 5$ cm. A Langmuir probe is scanned through the axial *z* direction biased to the electron saturation current. Measurements have been performed with the help of a boxcar averager. The microwave pulse width is adjusted at 90 ns and the gate for observing the signals is placed at the time $t = 0 - 13$ μs, where $t = 0$ is taken to be the time when the microwave pulse is turned off. One can observe a large density cavity at the resonance region near $z \simeq 32$ cm, after which pronounced plasma density perturbations are propagating down the density gradient. Let us present now the physical mechanism of exciting these large density perturbations. Due to the fundamental physics of the microwave-plasma interaction, the nonlinear ponderomotive force appearing at the resonant region can sweep out plasma electrons with a very high energy creating electron density dip, but leaving a bare ion column at the resonance layer. As a result this bare ion column in the resonant layer ideally can create a positive potential, which is also observed in our experiment as shown in Fig. 8. This figure shows the density cavity observed at the resonant region (bottom trace), corresponding positive space-potential (top trace), and schematic line of the density (middle trace) in the absence of microwave pulse. Whenever electrons are shot out from the resonant region by the ponderomotive force, a self-consistent ambipolar force pulls the ions producing an ion bunch [14–17], which travels through the underdense plasma column. This ion bunch acts as the driver to excite an ion wave-wake. These phenomena are the main topic of this paper. In the

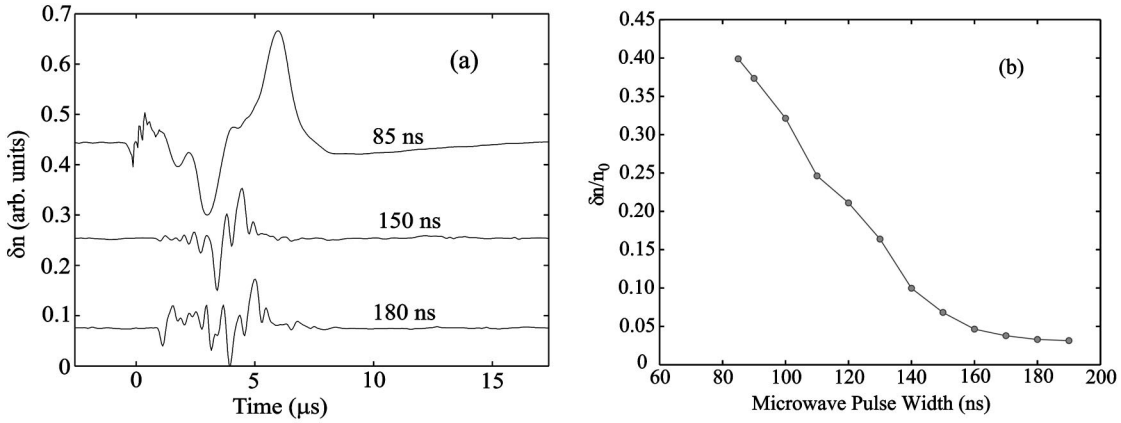

FIG. 6. (a) Temporal evolution of density perturbations (δn) with incident microwave pulse width of 85 ns, 150 ns, and 180 ns. (b) Amplitude variation of density perturbations ($\delta n/n_0 \equiv$ peak to peak value) as a function of the incident microwave pulse width.

present experiment the energy distribution of the ion bunch has been observed by a Faraday cup using first grid at the floating potential and second grid as an electron repeller. The first grid is used at the floating potential in order to repel back ground low energy plasma particles. The second grid is biased toword the negative voltage more than 150 volts until the electron flux vanishes from the collector signal. To analyze the ion energy spectrum, the positive retarding potential has been applied to the collector of the Faraday cup. Typical oscillogram of the energetic ion flux produced by the resonant absorption process is shown in Fig. 9(b), where one can see an ion bunch propagating down the density gradient. Energy distribution of the ion bunch is represented in Fig. 9(a). One can observe the maximal energy of a bunch of ions is about 58 eV. The top trace in Fig. 9(b) represents the incident microwave pulse, middle trace the excited wave form, and bottom trace a suprathermal ion bunch coming out from the resonant region.

While this suprathermal ion bunch travels down the underdense plasma column, it excites an ion wakefield as shown in Fig. 10. The wave forms are obtained by a Langmuir probe placed at different axial z positions with a fixed radial position $r \simeq 5$ cm. The pulse width of the incident microwave is set at 85 ns. The physical concepts of exciting ion wave by a driving bunch will be explained in the discussions (given in Sec. IV). The wave phase velocity ($v_{ph} \approx 1.8 \times 10^6$ cm/s) near the resonance layer is very close to the velocity of the ion bunch, which is measured by the energy analyzer near the resonance region. It is observed that the wave velocity as well as its amplitude damp rapidly in the vicinity of the resonant layer as shown in Fig. 11. After damping process has been achieved, the wave velocity ($v_{ph} \approx 5.6 \times 10^5$ cm/s) is found to be approximately twice the ion acoustic velocity ($c_s = 2.5 \times 10^5$ cm/s). Figures 11(a) and 11(b) show good matching between the variation of the wave phase velocity and the variation of its amplitude. In the experiment on the ion acoustic solitons, velocity of the solitons depends on its amplitude as $v \propto (\delta n/n_0)$ [18]. One can notice that the present results show a similar process of dependence of the velocity on its amplitude.

IV. DISCUSSIONS

This section reviews our results and describes various aspects of the resonant absorption and wakefield excitation by

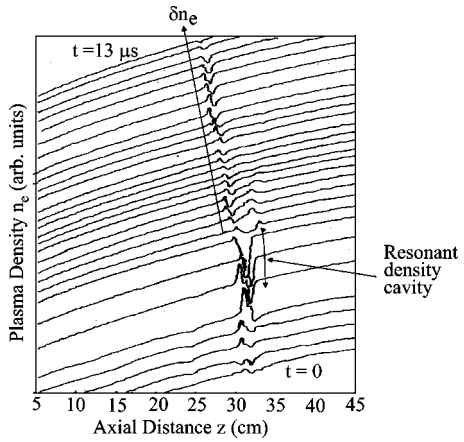

FIG. 7. Spatial profiles of plasma density n_e after irradiating the microwave pulse inside the plasma with pulse width 90 ns.

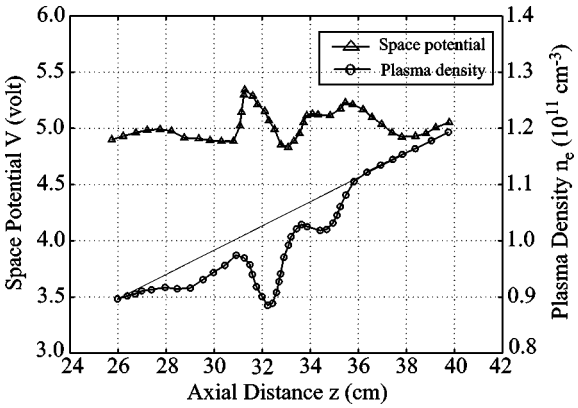

FIG. 8. Density cavity observed at resonant region (bottom trace), corresponding positive space-potential (top trace), and schematic line of density (middle trace) in the absence of microwave pulse.

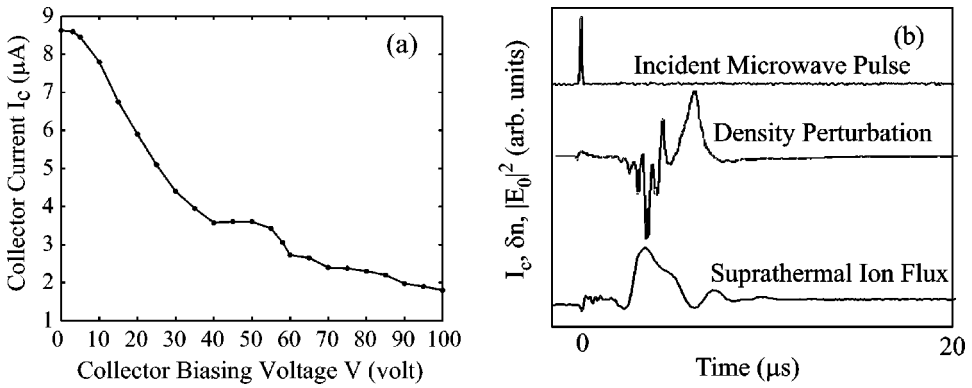

FIG. 9. (a) Ion energy resolution by a Faraday cup. (b) Incident microwave pulse (top trace), density perturbation (middle trace), and suprathermal ion flux (bottom trace).

an ion bunch ejected from the resonant absorption layer. When a *p*-polarized electromagnetic wave with $k_0 L_z \gg 1$ and amplitude E_0 is incident on a plasma slab with a linear density profile $n_e(z)=n_0[1+(z/L_z)]$ at an angle θ, then the localized electrostatic field developed in the resonant layer is given by $E_d=E_0\phi(\tau)/(2\pi k_0 L_z)^{1/2}$, where $\phi(\tau)$ is called Ginzburg function and $\tau=(k_0 L_z)^{1/3}\sin\theta$. In Sec. III, for calculating the angle of incidence θ Eq. (1) is derived by the following method. For the linear density profile and an incidence angle θ, the ray trajectories are assumed to be parabolic. The component of the group velocity in the radial (r) direction is constant. For a given microwave launch point z_l and the reflection (turning) point $z_T=L_z\cos^2\theta$, the radial deflection is proportional to the transit time τ_c from the point z_l to the point z_T. Thus one can calculate τ_c by the term $\tau_c=\int_{z_l}^{z_T} dz/(c\sqrt{1-\omega_p^2/\omega^2})$, which gives

$$\tau_c c=\int_{z_l}^{L_z\cos^2\theta}\left[1-\frac{z}{L_z}-\sin^2\theta\right]^{-1/2} dz \Rightarrow \tau_c c$$
$$=2L_z\left(\cos^2\theta-\frac{z_l}{L_z}\right)^{1/2}. \quad (2)$$

Substituting $r=\tau_c c\sin\theta$, we have

$$\frac{r^2}{(2L_z\sin\theta)^2}=\cos^2\theta-\frac{z_l}{L_z}, \quad (3)$$

which gives the solution expressed by Eq. (1) in Sec. III.

The nonlinear electrostatic field develops in the resonant region even for the modest nonlinear factor $\eta=E_0^2/4\pi n_e kT_e\approx 10^{-4}$ with a condition $E_d/E_0\gtrsim 1$. In the present experiment the parameter $\eta\approx 5.0\times 10^{-2}$ is used, which can create a high intensity nonlinear electrostatic field and develop a nonlinear ponderomotive force in the resonant plasma. This nonlinear ponderomotive force can sweep out electrons with a very high energy, creating electron density dip, but leaving a bare ion column at the resonance layer. These facts are described in Sec. III with Figs. 7 and 8. Whenever electrons are shot out from the resonant region by the ponderomotive force, a self-consistent ambipolar force can also pull out the ions from the resonant region as a bunch and can accelerate it through the underdense plasma column, which was experimentally demonstrated by Wong and Stenzel [15]. This bunch of ions can act as the driving bunch to excite an ion wave-wake behind it. In order to obtain large electric fields behind the driving bunch, in PWFA concept, it is necessary to cut the beam off within a time shorter than a plasma period [9]. The key result of the present experiment is that the pulse width of the incident microwave should be chosen as $\tau_{pi}\lesssim 2\pi/\omega_{pi}$, so that it can produce very small and sharp τ_{fall}. Note that in the experiment we have used $\tau_{fall}\lesssim\tau_{pi}$. Further reduction of the microwave pulse width leads to linear increase of the excited ion-wave amplitude. The dependence of the wave amplitude on the microwave pulse width has been shown in Fig. 6. In the experiment high energy ion bunch ($\simeq 58$ eV) is detected as shown in Fig. 9(a) and the excited wave form has been represented in Figs. 4 and 10.

The mechanism of excitation of an ion-wave wakefield by the supersonic ion bunch is described as follows. When a high energy ion bunch travels through the underdense plasma column, it can generate density perturbations. Defining the Fourier transform in space and Laplace transform in time by the following equations:

$$g(k)=\int_{-\infty}^{+\infty}\int_{-\infty}^{+\infty} dz\,dy\,\exp[i(k_z z+k_y y)]g(z,y),$$

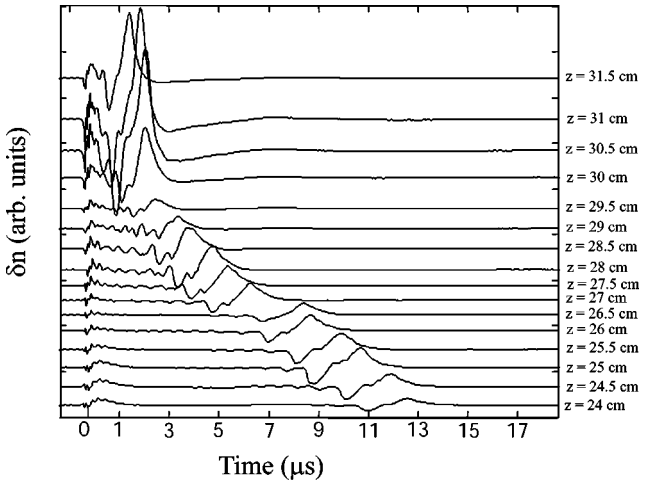

FIG. 10. Temporal evolution of the ion waves excited by suprathermal ion bunch taken at different underdense *z* positions at $r\simeq 5$ cm. In the measurements the incident microwave is irradiated with a pulse width 85 ns.

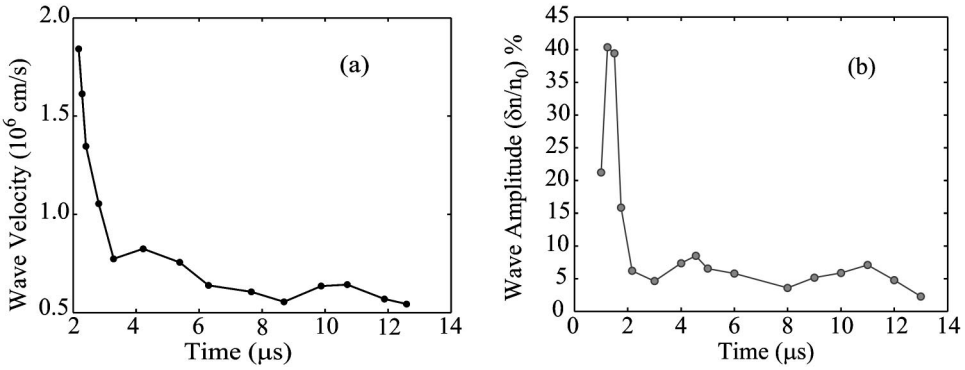

FIG. 11. (a) Temporal evolution of wave phase velocity. (b) Temporal evolution of wave amplitude.

$$f(\omega)=\int_0^\infty dt\,\exp(-i\omega t)f(t), \tag{4}$$

one can calculate the perturbed density generated by an ion bunch by the equation described as [17]

$$\tilde{n}(z,y,t)=\frac{1}{(2\pi)^3}\int dk_z\int dk_y\int d\omega\tilde{n}(k_z,k_y,\omega) \times\exp[-i(k_z z+k_y y)]\exp(i\omega t). \tag{5}$$

Let us locate the ion bunch arisen near the resonance region as $z\approx 0$ and $y\approx 0$ at $t=0$ and then propagation along z axis with the velocity v can be represented by

$$\delta n_{ext}(z-vt,y). \tag{6}$$

The density perturbation induced in the plasma by the imposed external perturbation $\delta n_{ext}(z-vt,y)$ can be written by the equation

$$\frac{\partial^2\tilde{n}}{\partial z^2}-\frac{1}{v^2}\frac{\partial^2\tilde{n}}{\partial t^2}=\frac{\partial^2}{\partial z^2}\delta n_{ext}(z,y,t). \tag{7}$$

This density perturbation can create space potential and can trap electrostatic wave and propagate along with the ion bunch.

To describe the wakefield excitation process due to the induced density perturbation propagating through the uniform plasma along z direction, let us consider Poisson's equation for the electric field E as $\partial E/\partial z=4\pi\rho$. Using double Fourier transform with the variable of spatial z and time t as

$$f(k,\omega)\equiv\int_{-\infty}^{+\infty}dz\int_{-\infty}^{+\infty}dt\,\exp[-i(kz-\omega t)]f(z,t), \tag{8}$$

one can find the wakefield expressed as [9]

$$E(k,\omega)=\frac{-4\pi i}{k}[\rho_p(k,\omega)+\rho_b(k,\omega)], \tag{9}$$

where ρ_p is induced plasma charge density and ρ_b is the charge density of the driving beam. Again using double Fourier transform charge density of the driving beam can be expressed as [9]

$$\rho_b(k,\omega)=2\pi\delta(\omega-kv)\int_{-\infty}^{+\infty}dy e^{iky}\rho_b(y), \tag{10}$$

where δ function selects the waves whose phase velocities is equal to the beam velocity. In the experiment, it is observed that near the resonant layer the phase velocity of the wave is nearly equal to the velocity of the ion bunch. However, the wave phase velocity as well as its amplitude damp rapidly in the vicinity of the resonant region as shown in Fig. 11. Since our plasma is inhomogeneous, the driving beam may defuse when it propagates from overdense to underdense direction. This geometrical diffusion of driving beam may cause the wave damping, resulting in the reduction of the wave amplitude as well as the velocity. Some other physical phenomena such as nonlinear Landau damping and trapping of particle in the wave potential-well may be another reason of this rapid damping.

V. CONCLUSIONS

We have excited the wakefield in the ion-wave regime by an ion bunch created by the resonant absorption process in a laboratory plasma. The resonant absorption is established by a high power short microwave pulse whose duration is of the order of $\tau_{pi}\lesssim 2\pi/\omega_{pi}$, incident obliquely in an inhomogeneous plasma. High energy ion bunch upto 58 eV has been detected. The excited wake propagates through the underdense plasma column with an initial high velocity 1.8×10^6 cm/s ($\simeq 7c_s$) and slows down to a velocity 5.6×10^5 cm/s which is approximately twice the ion acoustic velocity. Another physical process of sheath instability has been observed near the resonant region and the model of the instability is described.

ACKNOWLEDGMENTS

The present work was supported by a Grant-in-Aid for Scientific Research from the Ministry of Education, Sports and Culture, Science and Technology of Japan. One of the authors (M.S.) is grateful to Satellite Venture Business Laboratory (SVBL) at Utsunomiya University, INTAS (Grant No. YSF 00-93) and Russian Foundation for Basic Research (Grant No. 01-02-16675) for their financial support.

[1] T. Tajima and J.M. Dawson, Phys. Rev. Lett. **43**, 267 (1979).
[2] Y. Nishida, M. Yoshizumi, and R. Sugihara, Phys. Fluids **28**, 1574 (1985).
[3] Y. Nishida, N. Yugami, H. Onihashi, T. Taura, and K. Otsuka, Phys. Rev. Lett. **66**, 1854 (1991).
[4] Y. Nishida and T. Shinozaki, Phys. Rev. Lett. **65**, 2386 (1990).
[5] J.B. Rosenzweig, P. Schoessow, B. Cole, W. Gai, R. Konecny, J. Norem, and J. Simpson, Phys. Rev. A **39**, 1586 (1989).
[6] Y.B. Fainberg, V.A. Balakirev, I.N. Onishchendo, G.L. Sidelnikov, and G.V. Sotnikov, Fiz. Plazmy **20**, 674 (1994).
[7] P. Chen, J.M. Dawson, R.W. Huff, and T. Katsouleas, Phys. Rev. Lett. **54**, 693 (1985).
[8] J.J. Su, T. Katsouleas, J.M. Dawson, P. Chen, M. Jones, and R. Keinigs, IEEE Trans. Plasma Sci. **15**, 192 (1987).
[9] M.E. Jones and R. Keinigs, IEEE Trans. Plasma Sci. **15**, 203 (1987).
[10] Y. Nishida, T. Okazaki, N. Yugami, and T. Nagasawa, Phys. Rev. Lett. **66**, 2328 (1991).
[11] D.W. Aossey, J.E. Williams, H.S. Kim, J. Cooney, Y.C. Hsu, and K.E. Lonngren, Phys. Rev. E **47**, 2759 (1993).
[12] R.L. Stenzel, Rev. Sci. Instrum. **47**, 603 (1976).
[13] C. Rajyaguru, T. Fuji, H. Ito, N. Yugami, and Y. Nishida, Phys. Rev. E **64**, 016403 (2001).
[14] P. Koch and J. Albritton, Phys. Rev. Lett. **32**, 1420 (1974).
[15] A.Y. Wong and R.L. Stenzel, Phys. Rev. Lett. **34**, 727 (1975).
[16] N. Yugami, S. Kusaka, and Y. Nishida, Phys. Rev. E **49**, 2276 (1994).
[17] N. Yugami, S. Kusaka, Y. Nishida, B. Cros, and G. Matthieussent, Plasma Phys. Controlled Fusion **38**, 751 (1996).
[18] Y. Nishida, K. Yoshida, and T. Nagasawa, Phys. Fluids B **5**, 722 (1993).